Rotational Study of Carbon Monoxide Solvated with Helium Atoms

L. A. Surin,[1,2] A. V. Potapov,[1,2] B. S. Dumesh,[2] S. Schlemmer,[1] Y. Xu,[3] P. L. Raston,[3] and W. Jäger[3]

[1]*I. Physikalisches Institut, University of Cologne, 50937 Cologne, Germany*

[2]*Institute of Spectroscopy of RAS, 142190 Troitsk, Moscow Region, Russia*

[3]*Department of Chemistry, University of Alberta, Edmonton, Alberta, Canada T6G 2G2*

(Received 7 July 2008; published 3 December 2008)

High resolution microwave and millimeter-wave spectra of He_N-CO clusters with N up to 10, produced in a molecular expansion, were observed. Two series of $J = 1$–0 transitions were detected, which correspond to the a-type and b-type $J = 1$–0 transitions of He_1-CO. The B rotational constant initially decreases with N and reaches a minimum at $N = 3$. Its subsequent rise indicates the transition from a molecular complex to a quantum solvated system already for $N = 4$. For $N \geq 6$, the B value becomes larger than that of He_1-CO, indicating an almost free rotation of CO within the helium environment.

DOI: 10.1103/PhysRevLett.101.233401 PACS numbers: 36.40.Mr, 61.46.−w, 67.90.+z

Studies of helium (He) nanodroplets, which consist of 10^3–10^4 He atoms, have provided insight into the superfluid properties of He clusters with a characteristic size of several nanometers [1]. A fascinating fundamental question arose from these nanodroplet studies [2,3]: how many He atoms are required for the onset of superfluidity? To answer this question, small He_N-molecule clusters with $N \approx 2$–80 were recently explored using high resolution microwave (MW) and infrared (IR) spectroscopy [4–18]. Thus far, the He_N-OCS [4–8] and He_N-N_2O [9–11] systems were studied by both IR and MW spectroscopy, while He_N-CO_2 [12–14] and He_N-CO [15–17] were probed by IR and He_N-HCCCN [18] by MW spectroscopy.

A rather amazing effect has been observed for such small clusters, namely, an increase of the effective rotational constant B (proportional to the inverse moment of inertia) with increasing cluster size at a certain N. This nonclassical behavior has been interpreted as decoupling of part of the He density from the rotational motion of the molecule. It was proposed [4] that this decoupling is a sign of superfluidity at the microscopic level [4], in analogy to the ''macroscopic'' Andronikashvili experiment [19]. This was later corroborated by theory [10,20,21], and it now appears that the onset of superfluidity occurs in clusters with as few as 6 to 10 He atoms, depending strongly on the probe molecule.

Carbon monoxide, CO, is of special interest as a probe molecule. The He-CO dimer [22,23] has a binding energy (9 K) that is very close to the chemical potential of liquid He (7.5 K); CO is therefore a rather subtle probe of the surrounding He density. In the IR study of He_N-CO [15–17], two series of $R(0)$ transitions (a transition in which the rotational quantum number J changes from 0 in the vibrational ground state to 1 in the first excited vibrational state of CO) were observed. They were denoted as a- and b-types in analogy with He-CO, in which the a-type transition corresponds to end-over-end rotation of the whole complex, and the b-type corresponds to nearly free rotation of CO within the complex [22,23]. Theoretical simulations of the IR results [24,25] showed that the existence of two series at small N is likely due to a larger asymmetry of the cluster in this size regime and that the b-type series eventually disappears because of increasing cylindrical symmetry in larger clusters.

At the low jet temperature (< 1 K) only the lowest rotational level, $J = 0$, is significantly populated and mainly $R(0)$ transitions could be detected in the IR spectra of He_N-CO [15]. These data alone are insufficient to clearly separate the rotational frequency of the clusters from the shift of the fundamental vibration of CO. IR and theoretical studies of CO in He nanodroplets have also been reported [26]. The observed line broadening was attributed to coupling to phonons and droplet size distribution effects which are absent in the smaller He_N-CO clusters reported here. In that work, four isotopic species of CO were investigated in an effort to approximately separate the effects of vibration and rotation. However, a similar analysis applied to He_N-CO clusters gave scattered and inconsistent band shifts and rotational constants [17].

In this Letter, we present MW and millimeter-wave (MMW) measurements of pure rotational transitions of He_N-CO clusters in the range from $N = 2$ to 10. One goal is to elucidate the effect of a rather isotropic and shallow He-molecule potential on the spectroscopic properties of He_N-molecule clusters. The results will allow us to unambiguously separate the effects of rotation and vibrational shift on the spectra in order to detect possible nonclassical behavior of spectroscopic parameters.

Three different experimental techniques were used: a molecular beam Fourier transform microwave (FTMW) spectrometer [27] for detection of a-type transitions of clusters with $N = 2$–7 at 14–24 GHz; a MMW OROTRON intracavity jet spectrometer [28] for detection of b-type transitions with $N = 2$–10 at 114–150 GHz; and a MW-MMW double resonance (DR) technique combining the OROTRON spectrometer with a MW pump source [29] for detection of a-type transitions with $N = 7$–8 at

23–33 GHz. Both FTMW and OROTRON spectrometers use a resonant cavity as a sample cell providing extremely high sensitivity which is crucial for the present work. The principle of FTMW spectroscopy is based on the excitation of a molecular ensemble with a pulse of coherent radiation and the subsequent detection of the molecular emission signal [30]. The OROTRON spectrometer measures direct absorption and is based on an intracavity operation principle [31]. The DR technique was used to both confirm quantum number assignments and measure transitions which lie outside of the frequency range of these spectrometers. Here, the OROTRON spectrometer, adjusted to the frequency of the $J = 1$–0 b-type transition, serves as a sensitive detector of the population transfer induced by MW pump radiation in case of resonance with a corresponding $J = 1$–0 a-type transition.

The clusters were generated using pulsed pinhole supersonic jet expansions of very small amounts ($< 0.1\%$) of CO in He at backing pressures ranging from 10 to 80 atm. For the larger clusters, the jet nozzles were cooled to temperatures as low as $-80\,^{\circ}\mathrm{C}$ resulting in a rotational temperature in the gas expansion down to 0.1 K. The size ordering of the clusters was established by monitoring the signal intensity as a function of sample temperature, pressure, composition and by comparison with IR data. The DR technique allowed us to link the a- and b-type series of the $N = 7$ and 8 clusters, respectively, and confirmed the assignment made for two data sets from different techniques unambiguously.

The measured and assigned $J = 1$–0 transition frequencies are presented in Table I. They are also shown, together with the results of recent reptation quantum Monte Carlo calculations using the "CBS + corr" potential [25], in Fig. 1. The "CBS + corr" surface was obtained at the coupled-cluster level of theory with single, double, and full iterative triple excitations, using a complete basis set (CBS) [25]. The general agreement between the calculated and measured frequencies of the a-type series is good, but the calculated values for the b-type transitions are too high for $N = 3$–10, and experimental and calculated data diverge substantially for $N > 9$. The calculated intensities [25] of the a-type and b-type transitions show a monotonic increase and decrease, respectively, and correspond rather well to the experimentally determined intensities.

TABLE I. Measured frequencies of the $J = 1$–0 transitions of He_N-CO (in MHz).

N	a-type transitions	b-type transitions
1	17 277.7268	119 779.385
2	15 492.5636	127 234.352
3	14 475.8956	136 404.470
4	14 641.7260	144 173.088
5	15 808.9634	148 531.879
6	18 559.6605	149 836.536
7	23 760.3401	133 727.530 (154 557)[a]
8	32 053.4870	132 313.218
9		118 013.522
10		114 339.712

[a]Given in parentheses is the frequency of the upper component of the $J = 1$–0 transition of He_7-CO, as predicted from the IR data and data from the current study.

In the IR study, a limited number of split b-type $R(0)$ lines were observed, which show subtle differences among various isotopologues of CO in the range from $N = 4$ to 8 [15–17]. The most prominent splitting was found at $N = 7$ for all investigated CO isotopologues. At the same time, the theoretical procedure is not accurate enough to capture such fine details and presumably gives at best a weighted average of the split line positions [25]. Unfortunately, due to some small gaps in our frequency coverage, it was not possible to check the higher $J = 1$–0 b-type split component of the He_7-CO cluster. But detection of the lower frequency component and its position (see Fig. 1) confirms indirectly the splitting of this line at $N = 7$ in the IR spectrum. The disruption of the b-type series around $N = 7$ could be due to an avoided crossing with the ν_2 bending series moving down from around 5.39 cm^{-1} [15]. At $N = 15$, one further line splitting, this time in the a-type series, is seen in the experimental IR spectrum [15–17]. This N size region is not covered by the present study, but by extrapolating the observed tendency of the a- and b-type transitions to merge, one could imagine that the b-type transitions "cross" the a-type series around $N = 15$.

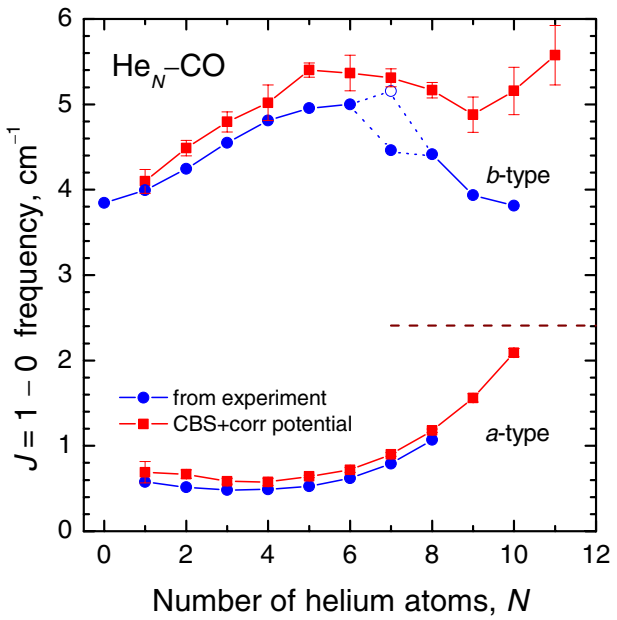

FIG. 1 (color online). Measured frequencies (●—filled circles) and those calculated from the CBS + corr potential (■—filled squares) [25] of the $J = 1$–0 transitions of the a-type and b-type series for the He_N-CO clusters. The frequency of the upper splitting component of He_7-CO (○—open circle) was estimated from the IR data [15] using the obtained vibrational shift. The dashed line indicates the $2B$ value inferred from the He nanodroplet experiments [26].

An important result of this study is the shift of the vibrational band origin of the He_N-CO clusters with respect to that of the free CO molecule (for He-CO, the band shift is -0.025 cm^{-1}). The vibrational shift was determined by subtracting the frequencies of the MW a-type transitions from corresponding frequencies of the IR lines [15], assuming that the a-type rotational frequency is the same in the lower and upper vibrational states. The result is shown in Fig. 2 together with the calculated data from the CBS + corr and symmetry-adapted perturbation theory (SAPT) potentials [25]. The dotted line is the inferred nanodroplet value [26]. For $N = 1$ to 8, the experimental band origins show a frequency shift to the red with an almost constant increment. This behavior is completely different from that of other dopant molecules, such as OCS, N_2O, and CO_2, where the band origin shows a constant frequency shift to the blue with each added He atom for $N = 1$ to 5. This blueshift indicates that the first five He atoms occupy equivalent positions forming a He "donut" around the equator of the doped molecule. With the addition of the next He atoms, the shift turns negative and leads toward its ultimate limiting value for He nanodroplets. The different behavior of the He_N-CO clusters can be related to the propensity of the He atoms to cluster at the oxygen end of carbon monoxide [24]. The observed sign and linearity of the shift of the He_N-CO cluster band origins is in qualitative agreement for this cluster size regime with recent theoretical simulation using the SAPT and CBS + corr potentials, but quantitatively much closer to the values from the CBS + corr potential. It is quite interesting to compare the vibrational shift to the inferred value from the nanodroplet measurements [26]. If the constant increment observed for the vibrational shift for $N = 1$–8 continues to larger N, then the inferred nanodroplet shift of -0.254 cm^{-1} would already be reached at $N = 10$, before filling of the first solvation shell at $N = 14$ [24]. Therefore, to attain its nanodroplet value, the vibrational shift must have a blue upturn at some larger N numbers or the band shift increment becomes smaller above $N = 8$.

The experimental effective rotational constants, B, are plotted in Fig. 3 as a function of cluster size N, with the inferred nanodroplet value [26] indicated by a dashed line. Since only $J = 1$–0 transitions were observed for each cluster size, the rotational constants were determined using a rigid symmetric top energy level expression with $K = 0$, i.e., $E = BJ(J + 1)$. Clusters with $N = 1, 2$ are asymmetric tops and the derived values correspond to $(B + C)/2$. This is also the case for larger clusters if there is a slight asymmetry in the helium density distribution. (Here, B and C are rotational constants of an asymmetric top molecule and are proportional to the inverse moments of inertia about the b- and c-principal inertial axes, respectively.)

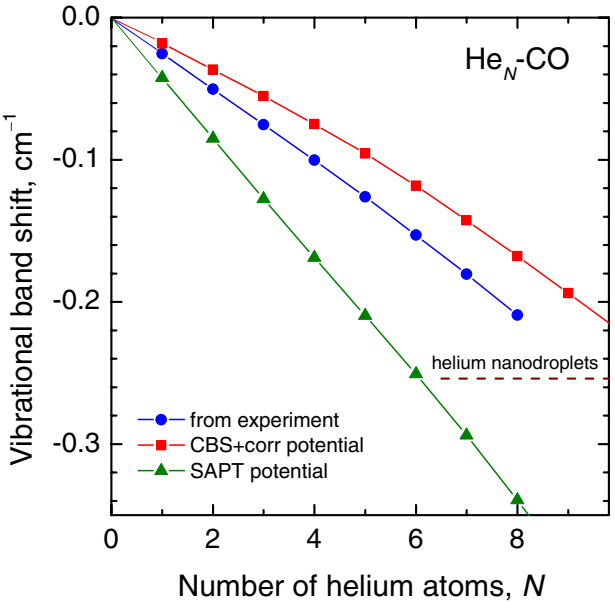

FIG. 2 (color online). Experimental (●—filled circles) frequency shift of the fundamental vibration of CO in the He_N-CO clusters. Theoretical simulations are from Ref. [25] using the CBS + corr potential (■—filled squares) and the SAPT potential (▲—filled triangles). The dashed line represents the inferred He nanodroplet value [26].

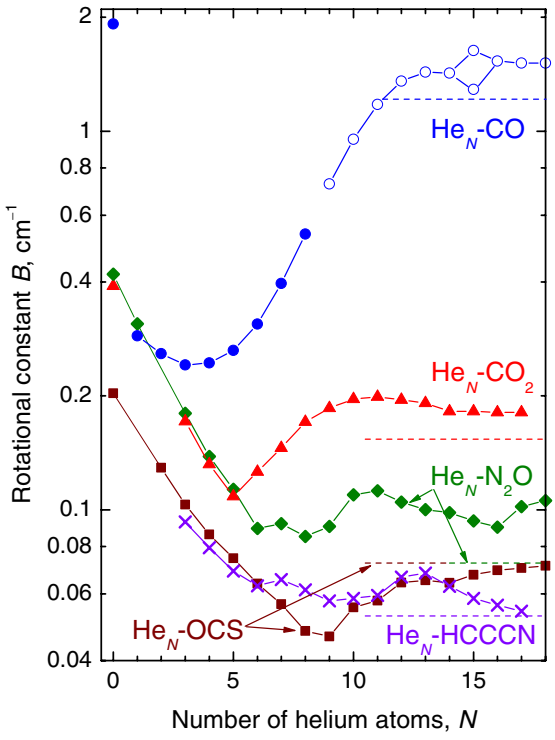

FIG. 3 (color online). Variation of rotational constant B with cluster size. Experimental values (●—filled circles) and those estimated from the IR spectra using the vibrational shift obtained in this work (○—open circles) are shown. The upper dashed line represents the inferred He nanodroplet limit [26]. For comparison, the corresponding plots for OCS [4–8], N_2O [9–11], CO_2 [12–14], HCCCN [18], and the corresponding nanodroplet values [2] are also shown. The B values are plotted on a logarithmic scale.

We estimate that the neglect of centrifugal distortion terms causes the B values to be at most 2% too low, by comparison with He_N-N_2O [10]. The B values for He_N-CO with $N = 1$–8 were directly obtained from the measured a-type transitions, while those for $N > 8$ were calculated from the IR data [15] assuming a constant increment of the vibrational shift with each He atom in the depicted size region. The main feature emerging is the B value turnaround at $N = 3$, at lower N than in all other probe molecules studied so far. The later turnaround of B vs N for the heavier molecules is likely due to their stronger and more anisotropic interactions with He [32]. A further significant difference from the corresponding plots for OCS, N_2O, CO_2, and HCCCN is the extremely small moment of inertia of the He_N-CO clusters, which becomes even smaller than the moment of inertia of the He_1-CO binary complex starting at $N = 6$. This means that the CO rotation is almost free and carries along the equivalent of less than one He atom in clusters with $N > 5$. Moreover, the observed spectra do not exhibit any additional line broadening, indicating that the relative motion of decoupled He density and probe molecule occurs without dissipation of energy.

The behavior of the B rotational constant indicates that part of the He density decouples from the rotational motion of the CO molecule and does not contribute to the moment of inertia of the cluster, thus signaling the transition from a molecular complex to a quantum solvated system. Following the idea that the decoupling of He density is a sign of superfluidy at the microscopic level [4], one can now state that superfluidity appears in clusters with as few as four He atoms. Feynman path-integral simulations have been used in the past to demonstrate that the decoupling between molecule rotation and helium motion is facilitated by particle exchange [10,21]. In other words, the nonclassical behavior of B vs N in He_N-molecule clusters is a consequence of permutation exchanges among ^{4}He atoms, and marks the onset of superfluid behavior in a finite system. Further experimental spectroscopic investigations of clusters involving fermionic particles, i.e., ^3He_N-molecule clusters, would unambiguously confirm if the turnaround in B is indeed an indicator of microscopic superfluidity. Such studies would help to clarify the relationship between ''microscopic'' and ''macroscopic'' superfluidity.

We thank A. R. W. McKellar and S. Moroni for stimulating discussions and F. Lewen for assistance with the DR measurements. We acknowledge the support by the Russian Foundation for Basic Research, by the Deutsche Forschungsgemeinschaft, and by the Natural Sciences and Engineering Research Council of Canada.

[1] S. Grebenev, J. P. Toennies, and A. F. Vilesov, Science **279**, 2083 (1998).
[2] J. P. Toennies and A. F. Vilesov, Angew. Chem., Int. Ed. **43**, 2622 (2004).
[3] F. Stienkemeier and K. K. Lehmann, J. Phys. B **39**, R127 (2006).
[4] J. Tang, Y. Xu, A. R. W. McKellar, and W. Jäger, Science **297**, 2030 (2002).
[5] Y. Xu and W. Jäger, J. Chem. Phys. **119**, 5457 (2003).
[6] J. Tang and A. R. W. McKellar, J. Chem. Phys. **119**, 5467 (2003).
[7] A. R. W. McKellar, Y. Xu, and W. Jäger, Phys. Rev. Lett. **97**, 183401 (2006).
[8] A. R. W. McKellar, Y. Xu, and W. Jäger, J. Phys. Chem. A **111**, 7329 (2007).
[9] Y. Xu, W. Jäger, J. Tang, and A. R. W. McKellar, Phys. Rev. Lett. **91**, 163401 (2003).
[10] Y. Xu, N. Blinov, W. Jäger, and P.-N. Roy, J. Chem. Phys. **124**, 081101 (2006).
[11] A. R. W. McKellar, J. Chem. Phys. **127**, 044315 (2007).
[12] J. Tang, A. R. W. McKellar, F. Mezzacapo, and S. Moroni, Phys. Rev. Lett. **92**, 145503 (2004).
[13] J. Tang and A. R. W. McKellar, J. Chem. Phys. **121**, 181 (2004).
[14] A. R. W. McKellar, J. Chem. Phys. **128**, 044308 (2008).
[15] J. Tang and A. R. W. McKellar, J. Chem. Phys. **119**, 754 (2003).
[16] A. R. W. McKellar, J. Chem. Phys. **121**, 6868 (2004).
[17] A. R. W. McKellar, J. Chem. Phys. **125**, 164328 (2006).
[18] W. Topic, W. Jäger, N. Blinov, P.-N. Roy, M. Botti, and S. Moroni, J. Chem. Phys. **125**, 144310 (2006).
[19] E. L. Andronikashvili, J. Phys. USSR **10**, 201 (1946).
[20] S. Moroni, A. Sarsa, S. Fantoni, K. E. Schmidt, and S. Baroni, Phys. Rev. Lett. **90**, 143401 (2003).
[21] F. Paesani, Y. Kwon, and K. B. Whaley, Phys. Rev. Lett. **94**, 153401 (2005).
[22] A. R. W. McKellar, Y. Xu, W. Jäger, and C. Bissonnette, J. Chem. Phys. **110**, 10 766 (1999).
[23] L. A. Surin, D. A. Roth, I. Pak, B. S. Dumesh, F. Lewen, and G. Winnewisser, J. Chem. Phys. **112**, 4064 (2000); **112**, 9190(E) (2000).
[24] P. Cazzato, S. Paolini, S. Moroni, and S. Baroni, J. Chem. Phys. **120**, 9071 (2004).
[25] T. Škrbić, S. Moroni, and S. Baroni, J. Phys. Chem. A **111**, 7640 (2007).
[26] K. von Haeften, S. Rudolph, I. Simanovski, M. Havenith, R. E. Zillich, and K. B. Whaley, Phys. Rev. B **73**, 054502 (2006); R. E. Zillich, K. B. Whaley, and K. von Haeften, J. Chem. Phys. **128**, 094303 (2008).
[27] Y. Xu and W. Jäger, J. Chem. Phys. **106**, 7968 (1997).
[28] L. A. Surin, B. S. Dumesh, F. Lewen, D. A. Roth, V. P. Kostromin, F. S. Rusin, G. Winnewisser, and I. Pak, Rev. Sci. Instrum. **72**, 2535 (2001).
[29] L. A. Surin, D. N. Fourzikov, F. Lewen, B. S. Dumesh, G. Winnewisser, and A. R. W. McKellar, J. Mol. Spectrosc. **222**, 93 (2003).
[30] T. G. Schmalz and W. H. Flygare, in *Laser and Coherence Spectroscopy*, edited by J. I. Steinfeld (Plenum, New York, 1978).
[31] B. S. Dumesh and L. A. Surin, Rev. Sci. Instrum. **67**, 3458 (1996).
[32] S. Paolini, S. Fantoni, S. Moroni, and S. Baroni, J. Chem. Phys. **123**, 114306 (2005).